

Formation of a two-dimensional $c(2 \times 2)$ Mn-Co(001) ferromagnetic surface alloy on Cu(001)

B.-Ch. Choi, P. J. Bode, and J. A. C. Bland

Cavendish Laboratory, Madingley Road, Cambridge CB3 0HE, United Kingdom

(Received 2 February 1998; revised manuscript received 8 April 1998)

The structure and magnetic properties of ultrathin Mn films on fcc Co/Cu(001) were studied at room temperature, using the *in situ* magneto-optical Kerr effect and low-energy electron diffraction. We found that a two-dimensional magnetic $c(2 \times 2)$ Mn-Co(001) surface alloy is stabilized in the range of 0.3–0.8 ML of Mn. Within this thickness range Mn is ferromagnetically coupled to the fcc Co(001) underlayer. Above one monolayer of Mn, the $c(2 \times 2)$ superstructure disappears and the Mn overlayer no longer has long-range ferromagnetic order. [S0163-1829(98)05533-7]

The magnetism of two-dimensionally ordered surface alloys based on transition metals, is currently of strong interest, providing important insight into magnetic interactions at the interface and the effects of the substrate on the magnetic ordering. A wide range of Mn surface alloys, based on Mn/Cu(001), Mn/Ni(001), and Mn/Fe(001),^{1–4} have been studied both theoretically and experimentally, both because of a rich variety of possible structural and magnetic phases occurring in epitaxially grown Mn films and because a large magnetic moment can form due to the half filled $3d$ shell of Mn. One of the most fascinating features of the Mn-based surface alloys is the $c(2 \times 2)$ superstructure, which has been observed by Wuttig, Gauthier, and Blügel⁵ in the MnCu surface alloy film on Cu(001) and which is found to be thermodynamically stable. They identified the magnetism of Mn atoms as the driving force for the stability of the alloy. The two-dimensional (2D) surface alloys are new magnetic materials, which provide possibilities for the preparation of very stable ultrathin films in the monolayer range and enable the experimentalist to perform well controlled experiments to test the theoretical predictions. The Mn/Co/Cu(001) structure provides a model epitaxial system which is well suited to the study of the magnetic interaction between Mn and ferromagnetic Co. Experimentally, O'Brien and Tonner⁶ have used x-ray magnetic circular dichroism (XMCD) to infer that a single Mn monolayer is ferromagnetically aligned with respect to the fcc Cu(001) film. However, competition between an in-plane antiferromagnetically ordered $c(2 \times 2)$ configuration and one in which a ferromagnetic Mn monolayer is antiferromagnetically coupled with respect to the Co underlayer is predicted by tight-binding model calculations.³ In this context it is important to note that any minor perturbation in the actual unit cell structure can have a potentially major influence on the magnetic properties given that the structural and magnetic energy contributions to the total energy are comparable in magnitude.

In this paper, we report the formation of a 2D $c(2 \times 2)$ MnCo magnetic surface alloy, where Mn is aligned ferromagnetically with respect to fcc Co/Cu(001). To our knowledge the existence of a MnCo magnetic surface alloy with the $c(2 \times 2)$ structure has not been previously reported. Moreover, we demonstrate that the formation of the $c(2 \times 2)$ MnCo surface alloy is clearly linked to the magnetic coupling of the Mn to Co underlayer at the Mn/Co interface.

The fcc Co(001) surfaces were prepared at room temperature under ultrahigh vacuum conditions by molecular beam epitaxy onto a Cu(001) single crystal at an evaporation rate of 1 ML/min. The base pressure is 1×10^{-10} mbar, and the pressure remains below 5×10^{-10} mbar during deposition.⁷ Throughout the experiment 8–9 ML of Co layers were deposited, because the Co film growth proceeds in a layer-by-layer growth mode above 2 and up to 10 ML.^{8,9} Auger electron spectroscopy (AES) measurements on the Co and Mn surfaces revealed no oxygen or carbon contamination at room temperature. Moreover, observation of the Auger signal as a function of time after Co deposition reveals no trace of Cu segregation on the Co surface within the detection limit (<0.3 ML), as is consistent with the report of Kief and Egelhoff,⁹ no surface segregation of the substrate Cu atoms was found after 6 ML of Co deposition. The 8–9 ML Co films still produce good (1×1) low-energy electron diffraction (LEED) patterns with a low background intensity, indicating that Co grows pseudomorphically on the Cu(001) substrate surface.¹⁰ Afterwards Mn overlayers up to 4 ML thickness were deposited on the fcc Co(001) surface at room temperature. The Co film thickness was determined by Auger electron spectroscopy and the Mn evaporation rate was calibrated by monitoring the $c(2 \times 2)$ LEED pattern formed at $\frac{1}{2}$ ML coverage of Mn on Cu(001).⁵ The formation of the MnCo surface alloys was determined by an ordinary LEED system. *In situ* magneto-optical Kerr effect MOKE was used to investigate the magnetic coupling of Mn to the fcc Co underlayer.

In the initial stage of Mn growth on the fcc Co(001) surface, the Mn grows epitaxially with the in-plane spacing and symmetry of fcc Co(001) and a sharp (1×1) LEED pattern was formed. Depositing 0.3 ML of Mn leads to the formation of faint $c(2 \times 2)$ superstructure spots in addition to the integer-order spots. As discussed above, the AES analysis allows us to verify that the superstructure does not come from the thermal segregation of Cu atoms at room temperature. With increasing Mn coverage the superstructure becomes more intense. In Fig. 1(a) we show a diffraction pattern at 136 eV obtained from 0.5 ML Mn on Co/Cu(001). The observed diffraction pattern is illustrated schematically in Fig. 1(b). We attribute this superstructure to the formation of the ordered MnCo surface alloy, stabilized by the magnetism of the Mn atoms. We assume that the mechanism for the

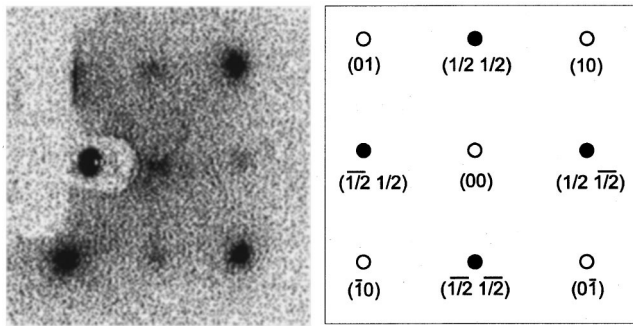


FIG. 1. (a) $c(2 \times 2)$ LEED pattern for 0.5 ML of Mn on fcc Co(001). The energy of primary electrons was set at 136 eV in order to make the extra spots visible, and so the (00) spot intensity is weak since this energy does not correspond to an in-phase scattering condition for the (00) spot. The integer order (10) and (01) spots are strongly overexposed to make the superstructure visible. (On the left-hand side of the photo the shadow of the sample holder and the LEED electron gun are also seen.) (b) Schematic representation of the observed LEED pattern. The open circles (integer-order beams) correspond to the fcc Co(001) spots and the filled small circles (half-order beams) are the $c(2 \times 2)$ spots.

formation of MnCo surface alloy is the outward buckling relaxation of the Mn atoms, as in the case of the CuMn surface alloy formed after deposition of ~ 0.5 ML Mn on the Cu(001) surface.^{5,11} However, we rule out the possibility that the interdiffusion of substrate Cu atoms through the Co film might lead to the formation of a MnCu surface alloy, since for Co layers above 6 ML thickness substrate interdiffusion can be neglected,⁹ and since the formation of $c(2 \times 2)$ structures was only observed promptly after 0.3–0.8 ML Mn deposition onto the Co surface. In support of this view, we find that the existence of the MnCo surface alloy correlates directly with the onset of ferromagnetic ordering in the Mn/Co/Cu(001) system, as will be discussed later in detail, whereas the MnCu surface alloy does not show any long-range magnetic order at room temperature.⁵

To obtain a better understanding of the formation of the MnCo surface alloy, the intensity of the $(\frac{1}{2} \frac{1}{2})$ spot in the $c(2 \times 2)$ LEED pattern was measured as a function of Mn coverage. In Fig. 2 we plot the $(\frac{1}{2} \frac{1}{2})$ extra spot intensity as a function of Mn thickness. A careful search by LEED revealed no detectable extra spots in the submonolayer Mn thickness range. The minimum thickness at which the $c(2 \times 2)$ structure is present is approximately 0.3 ML. At ~ 0.5 ML we found the maximum intensity of the $(\frac{1}{2} \frac{1}{2})$ beam, indicating that the 2D $c(2 \times 2)$ MnCo surface alloy is best ordered at this coverage. A rough estimation of surface roughness can be obtained from the spot profile analysis of the (10) and $(\frac{1}{2} \frac{1}{2})$ spots. At a primary beam energy of 136 eV we found that the half width of the (10) spot increases with Mn deposition, indicating an increase of the surface roughness with increasing Mn overlayer. At 0.5 ML Mn thickness, the half widths of the (10) and $(\frac{1}{2} \frac{1}{2})$ spots are found to be of the same magnitude ($\sim 12\%$ of the surface Brillouin zone along the [100] direction), indicating that the coherence lengths for $c(2 \times 2)$ and (1×1) long-range order are comparable in magnitude. With further growth of Mn, the superstructure intensities fall and finally disappear after deposition of a monolayer of Mn. We interpret this disappearance as the

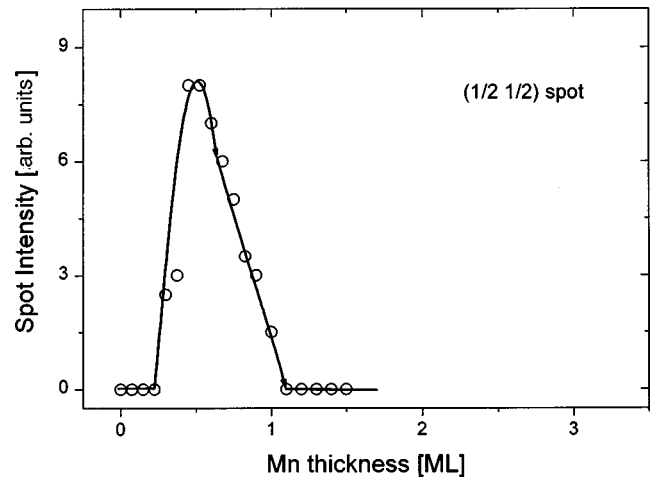


FIG. 2. Normalized LEED intensities of the $(\frac{1}{2} \frac{1}{2})$ beam in $c(2 \times 2)$ superstructure as a function of Mn thickness. The solid line is a guide to the eye.

completion of the first Mn layer, and we conclude that the Mn growth on the fcc Co surface occurs by a two-dimensional layer-by-layer growth mode rather than a three-dimensional island growth mode. If the Mn growth were to occur by an island growth mode, the $c(2 \times 2)$ structure should still be observable above 1 ML, which is not the case. After deposition of a monolayer of Mn, only the (1×1) spots remain, and the $c(2 \times 2)$ reconstruction of the Mn atoms disappears.

We now address the issue of how the formation of the MnCo surface alloy is related to the magnetic structure in the Mn/fcc Co(001) system. Figure 3 presents the Kerr signal (the saturated loop amplitude measured at 250 Oe magnetic field) as a function of Mn overlayer thickness, measured by *in situ* MOKE. For all measurements the magnetic field is applied along the [110] easy axis direction.¹² For coverages

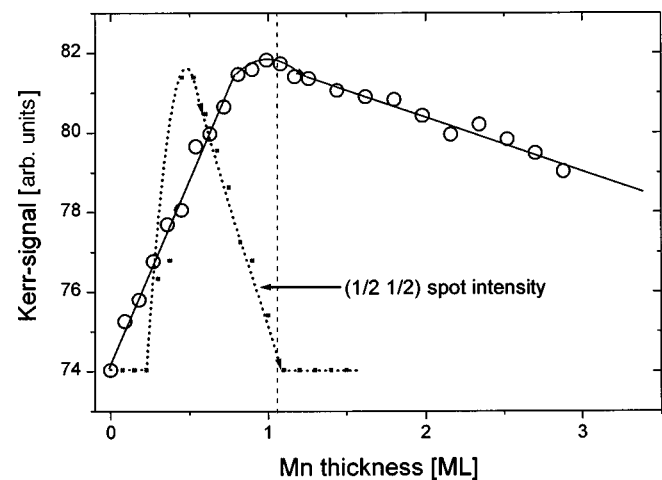


FIG. 3. The Kerr-signal (the saturated loop amplitude measured at 250 Oe magnetic field) as a function of the Mn thickness with the field applied along the [110] direction. The thickness dependent $c(2 \times 2)$ spot intensity (the dotted line) in Fig. 2 is also given to emphasize the correlation between the Kerr signal and the formation of the $c(2 \times 2)$ surface alloy. The lines are guides to the eye. The vertical dashed line divides the region with and without $c(2 \times 2)$ structure.

up to ~ 1 ML Mn, a monotonous increase of the Kerr signal is found, indicating that deposited Mn layers are all ferromagnetically ordered with respect to the Co substrate. This result is consistent with the experimental result by O'Brien and Tonner using XMCD,⁶ but is in contradiction with the recent theoretical study by Noguera *et al.*,³ who found antiferromagnetic coupling as the lowest-energy state for a monolayer of Mn deposited on the fcc Co(001) surface. This discrepancy could be partly due to the large outward relaxation of the Mn atoms on the surface alloy, as found on the Mn-Cu(001) surface alloy.⁵ This assumption is supported by theoretical studies of Mn impurities in Co,¹³ showing that the antiferromagnetic configuration is more stable than the ferromagnetic one, but only by a small energy difference of 0.12 eV. Hence the competition between both states might be easily changed by a small structural perturbation. Figure 3 shows, moreover, that there is a significant enhancement of the total sample magneto-optic signal induced even by depositing submonolayer quantities of Mn, indicating that there is a strong magnetic interaction between the Mn and the ferromagnetic Co underlayer. This result is in accordance with the report that the surface layer of Mn is in a high-spin state and has an enhanced local moment.⁶ A theoretical calculation for a monolayer of Mn on Ag(100) also yields a large moment of the order of $4\mu_B$.¹⁴ More importantly, the Mn thickness region for which ferromagnetic coupling of Mn to the Co layer occurs corresponds to the coverage where the $c(2\times 2)$ structure is ordered (Fig. 3). From this correlation we conclude that the ferromagnetic coupling is associ-

ated with Mn atoms in the $c(2\times 2)$ structure. After 1 ML of Mn, the Kerr signal begins to fall. Therefore, we can infer that above 1 ML thickness Mn the ferromagnetic behavior disappears; i.e., the Mn atoms in proximity to the Co underlayer couple ferromagnetically to Co, but subsequent Mn layers which are not in contact with the Co underlayer do not. In the phase having no long-range ferromagnetic order, no $c(2\times 2)$ superstructure was found and the (1×1) spots remain. This demonstrates that the surface alloy is stabilized by the magnetism of the Mn atoms and that the ferromagnetic coupling between Mn and Co is limited only to the Mn/Co interface.

In conclusion, we found evidence for the formation of a two-dimensional MnCo magnetic surface alloy in ultrathin Mn films grown on an fcc Co(001) surface. The observed $c(2\times 2)$ superstructure seen in the LEED pattern is attributed to the MnCo surface alloy. Corresponding to the two structural regions, we identified two magnetic phases of Mn; a ferromagnetic phase due to interfacial coupling of up to a monolayer of Mn, and a phase having no long-range ferromagnetic order above 1 ML of Mn. We demonstrate that the ferromagnetic coupling of Mn to the Co film is clearly linked to the formation of a two-dimensional MnCo surface alloy, located at the Mn/Co interface.

The financial support of the Engineering and Physical Sciences Research Council (EPSRC) and the British Council Alliance programs are gratefully acknowledged. We thank C. Demangeat for helpful discussions.

¹H. A. Dürr, G. van der Laan, D. Spanke, F. U. Hillebrecht, N. B. Brookes, and J. B. Goedkoop, *Surf. Sci.* **377**, 466 (1997).

²J. Dresselhaus, D. Spanke, F. U. Hillebrecht, E. Kisker, G. van der Laan, J. B. Goedkoop, and N. B. Brookes, *Surf. Sci.* **377**, 450 (1997).

³A. Noguera, S. Bouarab, A. Mokrani, C. Demangeat, and H. Dreyse, *J. Magn. Magn. Mater.* **156**, 21 (1996).

⁴W. L. O'Brien and B. P. Tonner, *Phys. Rev. B* **51**, 617 (1995).

⁵M. Wuttig, Y. Gauthier, and S. Blügel, *Phys. Rev. Lett.* **70**, 3619 (1993).

⁶W. L. O'Brien and B. P. Tonner, *Phys. Rev. B* **50**, 2963 (1994).

⁷S. Hope, E. Gu, B. Choi, and J. A. C. Bland, *Phys. Rev. Lett.* **80**, 1750 (1998).

⁸H. Li and B. P. Tonner, *Phys. Rev. B* **40**, 10 241 (1989).

⁹M. T. Kief and W. F. Egelhoff, *Phys. Rev. B* **47**, 10 785 (1993).

¹⁰J. J. de Miguel, A. Cebollada, J. M. Gallego, R. Miranda, C. M. Schneider, P. Schuster, and J. Kirchner, *J. Magn. Magn. Mater.* **93**, 1 (1991).

¹¹R. G. P. van der Kraan and H. van Kempen, *Surf. Sci.* **338**, 19 (1995).

¹²M. E. Buckley, F. O. Schumann, and J. A. C. Bland, *Phys. Rev. B* **52**, 6596 (1995).

¹³V. S. Stepanyuk, R. Zeller, P. H. Dederichs, and I. Mertig, *Phys. Rev. B* **49**, 5157 (1994).

¹⁴C. Fu, A. J. Freeman, and T. Oguchi, *Phys. Rev. Lett.* **64**, 673 (1985).